Branching ratio to the 803 keV level in ^{210}Po α decay

A. Shor,[1] L. Weissman,[1] O. Aviv,[1] Y. Eisen,[1] M. Brandis,[1] M. Paul,[2] A. Plompen,[3] M. Tessler,[2] and S. Vaintraub[1]

[1]*Soreq Nuclear Research Center, Yavne 81800, Israel*

[2]*Racah Institute of Physics, Hebrew University, Jerusalem 91904, Israel*

[3]*European Commission, Joint Research Centre, Retieseweg 111, B-2440 Geel, Belgium*

(Received 26 October 2017; published 2 March 2018)

Precise knowledge of the branching ratio in the α decay of ^{210}Po is important for accurate measurement of the ^{209}Bi$(n,\gamma)^{210g}$Bi cross section, the reaction involved in the termination of the astrophysical s process. The branching ratio was determined from independent measurements of α and γ spectra of bismuth samples simultaneously irradiated by neutrons near the core of the Soreq research reactor (IRR1). The branching ratio was found to be $(1.15\ \pm 0.09) \times 10^{-5}$, consistent with the results of several measurements performed six decades ago. As a by-product value the ^{209}Bi$(n,\gamma)^{210g}$Bi thermal cross section was measured to be 21.6 ± 1.1 mb.

DOI: 10.1103/PhysRevC.97.034303

I. INTRODUCTION

The ^{209}Bi isotope terminates the s process as the next neutron capture leads to the α unstable product ^{210}Po. Accurate knowledge of all measurements involved in stellar nuclear reactions and, in particular, the ^{209}Bi$(n,\gamma)^{210g}$Bi cross section is needed for reliable analysis of the s-process termination [1]. The neutron capture of bismuth has also a practical application since bismuth is considered to be suitable material for spallation targets and as a coolant for accelerator-driven systems. Therefore, the knowledge of the cross sections is essential for the radiation safety evaluation of future facilities.

Recent commissioning of the liquid lithium target (LiLiT) at the first phase of the Soreq Applied Research Accelerator Facility (SARAF) [2,3] prompted an astrophysical research program which also included measurements of Maxwellian-averaged cross sections (MACSs) of the ^{208}Pb$(n,\gamma)^{209}$Pb [4] and ^{209}Bi$(n,\gamma)^{210g}$Bi [5] reactions, playing a major role in the termination of the s process. An activation measurement is appropriate for the determination of the ^{209}Bi(n,γ) reaction cross section via the decays of the ^{210g}Bi ($T_{1/2} = 5.013$ days) and ^{210}Po ($T_{1/2} = 138.376$ days) isotopes (Fig. 1). In general, there are three methods to measure the cross section via such activation: (1) measurement of the β rays from the ^{210g}Bi decay, (2) measurement of the α-particle intensity in the ^{210}Po decay, and (3) measurement of the weak 803 keV γ ray in the ^{210}Po decay (Fig. 1). All three methods were utilized in a recent experiment [5]. γ-ray measurements performed with a high-purity germanium (HPGe) detector are reliable when good counting statistics are achieved. The result of the latter method will rely directly on the value of the weak branching ratio of the α decay to the 803 keV level in ^{206}Pb.

It is interesting to survey the literature on the experimental measurements of the branching ratio to the 803 keV level. There are quite a few measurements of the branching ratio [6–15]; however, all of them, except Ref. [15], were performed during the 1950s. Dramatic progress in nuclear radiation measurement instrumentation during the following 60 years makes it important to perform new measurements in order to confirm the literature results. In this respect it is worthwhile to emphasize that the result of the recent work of Ref. [15] [$(0.88\ \pm 0.05) \times 10^{-5}$] is lower by almost 40% than the most recent recommended value [$(1.23 \pm 0.04) \times 10^{-5}$] [16] based on the results of the earlier experiments [6–13]. Determination of the branching ratio is also of special importance in the context of our recent work for the determination of the ^{209}Bi$(n,\gamma)^{210g}$Bi MACS [5].

II. IRRADIATION

The experiment involved simultaneous neutron irradiation of two pure bismuth samples near the core of the Soreq IRR1 research reactor. The samples were placed and underwent irradiation with essentially identical neutron fluence. One sample is a thin foil to be used after irradiation for α spectrometry; another is a much thicker disk to be used for γ-ray measurements.

The target foil consists of a 1-μm-thick bismuth layer with nominally 99.97% pure bismuth sputtered onto a 0.25-mm Mylar foil, acquired from Evochem GmbH [17]. The bismuth foil was punched out with a precise 8-mm-diam punch. The thickness of the foil was measured using Rutherford backscattering (RBS) techniques with a 3 MeV He^+ beam at the Bar-Ilan ion-beam analysis laboratory [18] and was found to be of $(2.86 \pm 0.12) \times 10^{18}$atoms/cm^2 (see Ref. [5] for more details). The uncertainty in the punch diameter was conservatively estimated as 0.1 mm, which corresponded to an additional 2.5% uncertainty in the foil area.

A 1-mm-thick bismuth plate of 99.9999% was purchased from Princeton Scientific [19]. An 8-mm-diam disk was punched out of the plate using the same precise punch. Since the bismuth plate was very brittle it was sandwiched between two aluminum plates during the punching process. The thick bismuth disk was weighed at 0.5302 ± 0.0005 g, or $1.527 \pm 0.002 \times 10^{21}$ atoms.

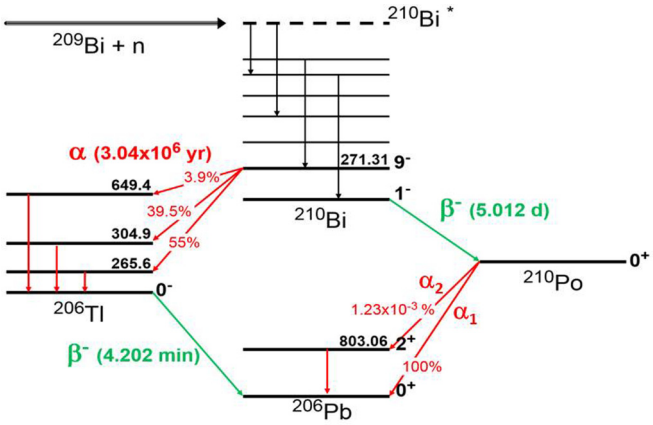

FIG. 1. The processes involving neutron capture of ^{209}Bi. The branching ratio of ^{210}Po α decay to the 803 keV state is taken from Ref. [16].

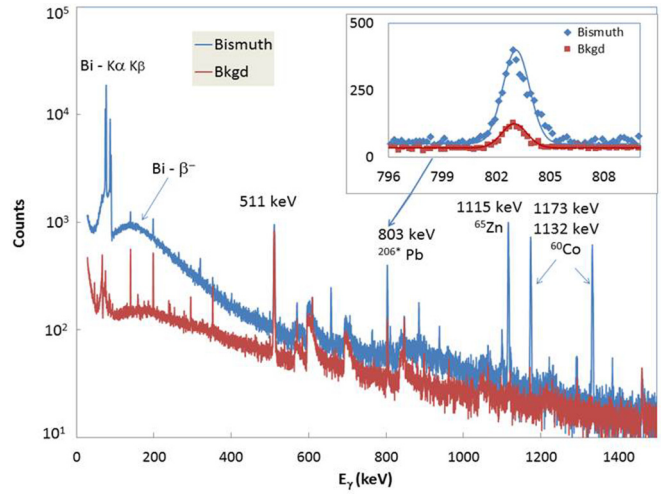

FIG. 2. γ spectrum from measurement of irradiated 1-mm-thick bismuth target in a low background shielded HPGe. Background spectrum normalized to the same live time as the bismuth spectrum is also shown. A zoom-in on the 803 keV peak is shown in the inset.

The thin and thick bismuth samples were gently sandwiched together, placed in a quartz ampule, and put into the pneumatic system (rabbit) in the Soreq reactor and irradiated for 20 min. The expected neutron fluence rate at the irradiation position is of the order of $10^{12}\,n\,\mathrm{cm}^{-2}\mathrm{s}^{-1}$ and the cadmium ratio with respect to gold standard, i.e., the ratio of thermal to epithermal and fast neutrons, is estimated as 8 ± 1. Since the measurement is based on the ratio of activation of the two samples, the experimental result for the branching ratio is independent of the neutron flux. Nevertheless, efforts were made for quantitative evaluation of the neutron fluence. A $6.0 \pm 0.1\,\mathrm{mg/cm}^2$ thick gold foil of 8 mm diameter was also irradiated together with the two bismuth samples for determination of the neutron fluence.

III. MEASUREMENTS AND ANALYSIS

A. γ measurements

After extraction of the ampule from the reactor core, the samples were allowed to decay for a 2.5-week period. The measurement of the activity from the irradiated gold sample was performed using a well-calibrated HPGe detector with 25% relative efficiency. The spectrum was taken with the sample placed at a distance of 20 cm from the detector. The detection efficiency of the 411.8 keV γ ray from the ^{198}Au decay was $0.145 \pm 0.005\%$ at this distance. The total neutron flux was corrected for the detector efficiency, branching ratio, and decay losses in order to obtain the number of ^{198}Au nuclei produced in the irradiation. Based on this measurement and the gold activation cross section of the $^{197}\mathrm{Au}(n,\gamma)^{198}\mathrm{Au}$ reaction for thermal neutrons of $\sigma = 98.65$ b, one can evaluate the flux of thermal neutrons irradiating the bismuth samples, found to be $2.5 \times 10^{12}\,n\,\mathrm{cm}^{-2}\mathrm{s}^{-1}$. This corresponds to a total of 1.9×10^{15} thermal neutrons irradiating the bismuth samples. Corrections for the resonance integral are small given the cadmium ratio of $\sim$8 at the "rabbit" location; however, this does not affect the branching ratio we aimed to determine.

Knowing the fluence of thermal neutrons, the number of ^{209}Bi nuclei and the number of produced ^{210g}Bi nuclei (N^a_{Bi210}, see below) in the thin sample allows one to deduce the value of the $^{209}\mathrm{Bi}(n,\gamma)^{210g}\mathrm{Bi}$ cross section for thermal neutrons. The deduced value of $\sigma = 21.6 \pm 1.1$ mb is in good agreement with the literature [20].

γ-ray measurement of the thick bismuth sample was performed following a longer cooling period of 42 days after the irradiation, sufficient time for most (99.7%) of the ^{210g}Bi to decay to ^{210}Po. The measurement of the 803 keV γ ray was performed over a period of about 9 days. The γ measurements were done in contact with a shielded 70% p-type coaxial HPGe detector (model GEM 65-83, ORTEC [21]). The HPGe detector was shielded by 10 cm of ordinary lead and 5 cm of low background lead (2.8 Bq/kg) as well as a 3-mm low activity tin liner. In addition, a 100 cm $\times$ 100 cm $\times$ 5 cm scintillator was used in anti-coincidence with the HPGe detector for reduction of background signals caused by cosmic rays. The background level inside the shielded detector was about three orders of magnitude lower than typical unshielded surface γ background. This low background was necessary for clear identification of the 803 keV peak given the low ($\sim 10^{-5}$) branching ratio for this decay scheme. Detector efficiency for 803 keV with the bismuth sample in contact with the detector was determined to be $6.96 \pm 0.020\%$, using a calibrated multiline γ source (46–1836 keV). Monte Carlo simulations were performed using the GEANT4 simulation code [22] for a consistency check of the determined efficiency and for accurate assessment of finite sample size and bismuth self-absorption of the 803 keV γ rays. A separate measurement of the HPGe background was also performed for background subtraction. Despite the shielded low background environment, a faint signal around the 803 keV line from the natural background contribution of polonium was present. Figure 2 shows the γ spectrum obtained from the measurement of the irradiated thick bismuth disk, with a comparison of the low-level background spectrum collected over $\sim$9 days and properly normalized to the measurement live time of the bismuth sample spectrum. The section of the γ spectrum in the region of the

803 keV peak from the $^{210}\mathrm{Po}\rightarrow{}^{206*}\mathrm{Pb}+\alpha\rightarrow{}^{206}\mathrm{Pb}+\gamma_{803}$ decay is shown in the figure inset. The γ line shape shown in the inset slightly deviates from a Gaussian on the high-energy side. The strong γ lines in the spectrum all exhibit a similar feature in their line shape. This effect was due to slight drift of the HPGe amplifier gain during the 9 days' measurement. A linear background was assumed before and after the peak. The number of counts in the peak region above the linear fit of background gave the number of counts in the 803 keV peak. Additional features associated with the activated sample are lines from the bismuth x rays and β continuum and some γ rays from contaminants, the strongest of which are ^{65}Zn and ^{60}Co isotopes (Fig. 2). The number of counts in the 803 keV peak, minus the background contribution, was found to be

$$S_\gamma^{\mathrm{meas}} = 2513 \pm 113.$$

The number of activated ^{210g}Bi atoms at the end of irradiation, $N_{\mathrm{Bi210}}^{\gamma}$, is determined from the counts measured in the 803 keV γ peak, S_γ^{meas}:

$$S_\gamma^{\mathrm{meas}} = N_{\mathrm{Bi210}}^{\gamma}\left[\frac{\lambda_\alpha\lambda_\beta}{\lambda_\beta-\lambda_\alpha}\right]t_{\mathrm{live}}\varepsilon_\gamma\gamma_{\mathrm{b.r.}}\gamma_{\mathrm{bi\text{-}abs}}\gamma_{\mathrm{el\text{-}conv}} \times\left[f_{\mathrm{meas}}^{\alpha}\exp(-\lambda_\alpha t_{\mathrm{cool}})-f_{\mathrm{meas}}^{\beta}\exp(-\lambda_\beta t_{\mathrm{cool}})\right], \quad (1)$$

where t_{cool} is the cooling time from the end of irradiation until the beginning of measurement (42 days), t_{meas} is the measuring time (9.02 days), and t_{live} is the live time (8.98 days) of the measurement. $\lambda_\beta = \ln(2)/\tau_\beta$ ($\tau_\beta = 5.013$ days) is the decay constant of $^{210gs}\mathrm{Bi}\rightarrow{}^{210}\mathrm{Po}+\beta^-$, and $\lambda_\alpha = \ln(2)/\tau_\alpha$ ($\tau_\alpha = 138.376$ days) is the decay constant of $^{210}\mathrm{Po}\rightarrow{}^{206}\mathrm{Pb}+\alpha$. $\varepsilon_\gamma = 0.0696 \pm 0.0020$ is the detection efficiency. $\gamma_{\mathrm{b.r}}$ is the branching ratio for $^{210}\mathrm{Po}\rightarrow{}^{206}\mathrm{Pb}^*+\alpha\rightarrow{}^{206}\mathrm{Pb}+\gamma$ and the 803 keV γ line, which are determined in this work. The correction for electron conversion is taken from Ref. [14] and is given by $\gamma_{\mathrm{el\text{-}conv}} = 0.9920 \pm 0.0002$. The γ self-absorption correction for the 1-mm bismuth sample placed in direct contact with the HPGe detector was determined by detailed GEANT4 simulations to be $\gamma_{\mathrm{bi\text{-}abs}} = 0.886 \pm 0.001$. The quantities $f_{\mathrm{meas}}^{\alpha}$ and $f_{\mathrm{meas}}^{\beta}$ are the corrections for the finite measuring time and are given by $f_{\mathrm{meas}}^{\beta} = \frac{1-e^{-\lambda_\beta t_{\mathrm{meas}}}}{\lambda_\beta t_{\mathrm{meas}}}$ and $f_{\mathrm{meas}}^{\alpha} = \frac{1-e^{-\lambda_\alpha t_{\mathrm{meas}}}}{\lambda_\alpha t_{\mathrm{meas}}}$, where $f_{\mathrm{meas}}^{\beta}$ was found to be 1.001, while $f_{\mathrm{meas}}^{\alpha}$ was about 1.0226. Decay correction during irradiation was negligible given the short irradiation time (20 min) with respect to the half-life (138.3 days).

To treat properly the time dependence, we introduce for both γ and α (see below) the effective maximum activities A_γ and A_α, which correspond to the maximum activity at the end of irradiation if it were only a one-step decay process. The effective maximum γ activity A_γ is then given by the following formula:

$$A_\gamma = \frac{S_\gamma^{\mathrm{meas}}}{t_{\mathrm{live}}\varepsilon_\gamma\gamma_{\mathrm{bi\text{-}abs}}\gamma_{\mathrm{el\text{-}conv}}\left[f_{\mathrm{meas}}^{\alpha}\exp(-\lambda_\alpha t_{\mathrm{cool}})-f_{\mathrm{meas}}^{\beta}\exp(-\lambda_\beta t_{\mathrm{cool}})\right]} = 0.0675 \pm 0.0035\ \mathrm{Bq}. \quad (2)$$

The effective maximum γ activity is related to the number of activated ^{210g}Bi atoms at the end of irradiation as

$$A_\gamma = N_{\mathrm{Bi210}}^{\gamma}\left[\frac{\lambda_\alpha\lambda_\beta}{\lambda_\beta-\lambda_\alpha}\right]\gamma_{\mathrm{b.r.}}. \quad (3)$$

B. α measurement

The α spectrum, obtained from the thin bismuth sample, was measured with a passivated implanted planar silicon (PIPS) detector in a commercial shielded measuring system (Canberra model iSolo500 [23]). The PIPS detector has an active area of 2000 mm^2 and an active thickness of 500 μm. The measurement was started soon after a 2.5-week cooling period, corresponding to decay of ~90% of the ^{210g}Bi component. The detection efficiency of the iSolo system was determined from a calibrated triple α source (Eckert and Ziegler [24]) with α lines centered at energies of 5.1, 5.5, and 5.8 MeV originating from the ^{239}Pu, ^{241}Am, and ^{244}Cm isotopes, respectively. These energies are close to the ^{210}Po α energy of 5.3 MeV. The calibration source diameter of 7 mm is very similar to that of the bismuth foil (diameter of 8 mm). The activities of the radionuclides in the calibration source are known to within an accuracy of ±1.5%. A pulse height threshold of 2 MeV-equivalent (taking into account energy loss in the air) was used to reject β contribution (see Fig. 3). The measured α efficiency over the relevant area was (36.5 ± 0.7)%. We assumed that the same fraction of α particles were below threshold also for the thin bismuth sample and for the calibration source (Fig. 3).

The sample was placed on a tray at a distance of 7.8 mm beneath the detector. The 8-mm-diam bismuth foil was well within the 50-mm-diam area of the PIPS detector. The measuring compartment was not in vacuum; therefore, multiple scattering and energy loss affected the distribution of α and β particles. The relatively large solid angle resulted in a large angle distribution of the outgoing α particle from the irradiated foil and, hence, caused additional broadening. Figure 3 shows an example of the measured α and β spectrum of the irradiated bismuth sample (red curve), together with the α spectrum of the calibration triple α source (black curve).

The first set of measurements was carried out over a period of a month. In order to achieve a better time base for the buildup-decay fit, an additional set of measurements was taken after a waiting period of 3 months. The dependence of the α-particle activity on time following irradiation of the bismuth foil is shown in Fig. 4. The data points represent the average α-particle activity per 12-h measuring period obtained by taking the integral counts in the α region of the spectra, divided by the measurement time, and corrected for the α-particle detection efficiency. The parameter t is the elapsed time from the end of irradiation until the middle of the activity measurement. The dependence of the α-particle activity can be described using

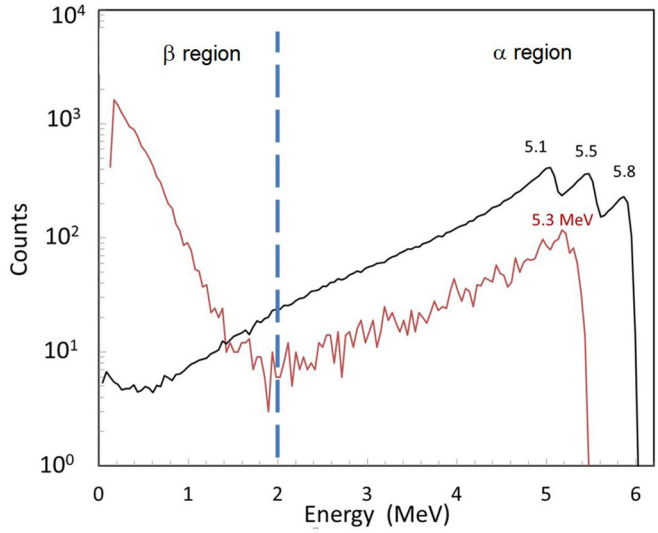

FIG. 3. Example of spectrum obtained from the irradiated thin bismuth sample (red line) taken 40 days after the irradiation. The spectrum of the calibrated triple α source is also shown (black line). The vertical dashed line represents the threshold used to distinguish between events originating from α and β particles.

the following function:

$$A_\alpha(t) = N^{\alpha}_{\mathrm{Bi210}}\left[\frac{\lambda_\beta\lambda_\alpha}{\lambda_\beta-\lambda_\alpha}\right][\exp(-\lambda_\alpha t)-\exp(-\lambda_\beta t)], \quad (4)$$

where $\lambda_\beta = \ln(2)/\tau_\beta$ is the decay coefficient of $^{210\mathrm{gs}}\mathrm{Bi}\rightarrow{}^{210}\mathrm{Po}+\beta^-$, and $\lambda_\alpha = \ln(2)/\tau_\alpha$ is the decay coefficient of $^{210}\mathrm{Po}\rightarrow{}^{206}\mathrm{Pb}+\alpha$. The decay corrections during the irradiation and measurements are negligible since these periods were significantly shorter than the half-life. The excellent fit, shown in Fig. 4, is an indication that there were no significant contributions from other α-particle-emitting radioisotopes in the sample as well as supporting the assumption of constant measurement parameters. A similar analysis of the β activity exhibited significant deviation from

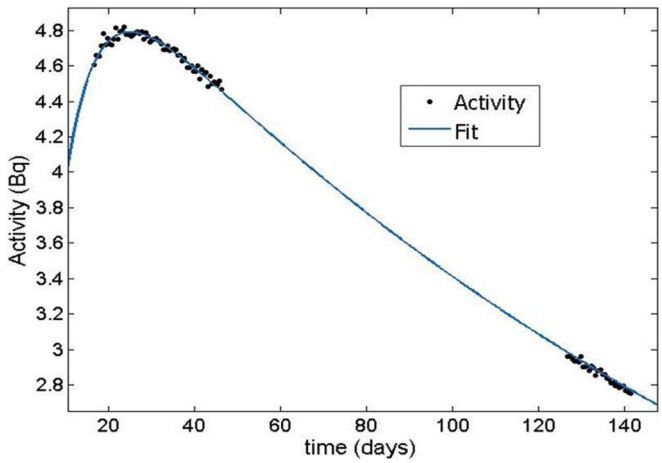

FIG. 4. ^{210}Po activity from α measurements of the irradiated bismuth foil as a function of time since irradiation. The solid blue line is a fit using Eq. (4).

TABLE I. Summary of the main contributing uncertainties.

Source of uncertainty	Uncertainty (%)
803 keV peak statistical error	4.5
Number of atoms in the thin sample (RBS measurement)	4.1
803 keV γ-ray detection efficiency	2.9
Number of atoms in the thin sample (area error)	2.5
α detection efficiency	1.5
Fit of α decay	1.0
Number of atoms in the thick sample (weighting error)	0.1
Total	7.5

the expected buildup-decay trend, most likely due to the presence of other β-particle-emitting radionuclides in the sample. Therefore, the β activity measurements were not used in the determination of the branching ratio.

In order to remove time dependence for a more straightforward comparison with the γ measurement, we determine the effective maximum α activity given by

$$A_\alpha = N^{\alpha}_{\mathrm{Bi210}}\left[\frac{\lambda_\beta\lambda_\alpha}{\lambda_\beta-\lambda_\alpha}\right] = 5.55\ \pm 0.10\ \mathrm{Bq}. \quad (5)$$

The main contributions to the uncertainty in A_α are associated with the α-detection efficiency (1.5%) and the fit error (1%).

IV. DISCUSSION

The γ activity is compared to the α activity, allowing one to extract the branching ratio for intermediate α decay to $^{206}\mathrm{Pb}^*$ compared to direct α decay to ^{206}Pb. Since the thick bismuth disk and the thin bismuth foil were adjacent to each other during activation, the ratio of activated ^{210}Bi nuclei, and correspondingly the intermediate ^{210}Po nuclei, should be proportional to the number of bismuth atoms contained in each of these samples [using Eqs. (3) and (5)], i.e.,

$$\frac{N^{\gamma}_{\mathrm{Bi210}}}{N^{\alpha}_{\mathrm{Bi210}}} = \frac{N^{\mathrm{thick}}_{\mathrm{Bi209}}}{N^{\mathrm{foil}}_{\mathrm{Bi209}}} = \frac{\frac{A_\gamma}{\left[\frac{\lambda_\alpha\lambda_\beta}{\lambda_\beta-\lambda_\alpha}\right]\gamma_{\mathrm{b.r.}}}}{\frac{A_\alpha}{\left[\frac{\lambda_\beta\lambda_\alpha}{\lambda_\beta-\lambda_\alpha}\right]}} = \frac{1}{\gamma_{\mathrm{b.r.}}}\frac{A_\gamma}{A_\alpha}.$$

Thus, the measured value for the branching ratio of $^{210}\mathrm{Po}\rightarrow{}^{206}\mathrm{Pb}^*+\alpha\rightarrow{}^{206}\mathrm{Pb}+\gamma$, as compared to $^{210}\mathrm{Po}\rightarrow{}^{206}\mathrm{Pb}+\alpha$, is then

$$\gamma_{\mathrm{b.r.}} = \frac{A_\gamma}{A_\alpha}\frac{N^{\mathrm{foil}}_{\mathrm{Bi209}}}{N^{\mathrm{thick}}_{\mathrm{Bi209}}} = \frac{0.0675\pm0.0035}{5.55\pm0.10}\frac{(1.44\pm0.07)\times10^{18}}{(1.527\pm0.002)\times10^{21}}$$
$$= (1.15\ \pm0.09)\times10^{-5}$$

The main contributions in the experimental error are listed in Table I. As can be seen from the table, the main contribution to the experimental error is associated with counting statistics of the 803 keV γ ray and uncertainty in the determination of the number of bismuth atoms in the thin sample.

The obtained result for the branching ratio is shown in Fig. 5 and Table II together with the results from the literature [6–15] and the most recent evaluations [16,25,26]. Most of the earlier experiments [6–13] were based on direct measurement of the

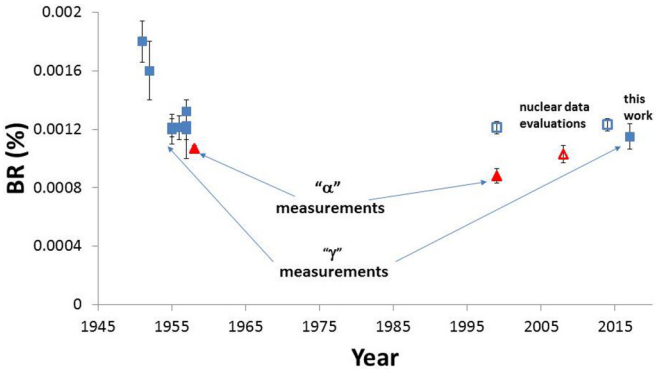

FIG. 5. The result of the present measurement is compared with the literature [6–15] and the most recent nuclear data evaluation [16,25,26]. The solid squares ([6–13], and the present work) are the experimental results of the direct measurements of the 803 keV γ ray. The solid triangles are the experiments based on direct measurement of the weak α_2 branch [14,15]. The open squares [16,25] and the open triangle [26] are the nuclear data evaluations of the γ-ray and α-ray experiments, respectively. See Table II and text for details.

TABLE II. Summary of the experimental results. The "γ" measurements are based on direct measurement of the 803 keV γ ray, while the "α" measurements rely on measurement of the weak α_2 branch.

Year	Result (%)	Reference	Method of measurement
1951	0.00180(14)	[6]	γ
1952	0.0016(2)	[7]	γ
1955	0.00121(6)	[8]	γ
1955	0.0012(1)	[9]	γ
1956	0.00121(8)	[10]	γ
1957	0.0012(2)	[11]	γ
1957	0.00122(9)	[12]	γ
1957	0.00132(8)	[13]	γ
1958	0.00107(2)	[14]	α
1999	0.00088(5)	[15]	α
1999	0.00121(4)	[25]	Evaluation of the γ experiments
2008	0.00103(6)	[26]	Evaluation of the α experiments
2014	0.00123(4)	[16]	Evaluation of the γ experiments
2017	0.00115(9)	This work	γ

803 keV γ ray, while the direct measurement of the ratio of the α_1 and α_2 intensities (Fig. 1) was performed in Refs. [14,15]. The recent evaluations [16,25] adopted the results obtained in the direct γ measurements, while the nuclear data evaluation [26] adopted the branching ratio obtained from the direct α measurements. It is worthwhile to note that there is a significant difference between the results of the two types of measurements and the corresponding evaluations (Fig. 5 and Table II). This difference is probably due to the difficulties in measurement of the extremely weak α_2 branch. The nuclear data evaluations based on direct measurements of the γ ray [16,25] provide the recommended value for the decay branching ratio.

The method used in this work utilizes measurement of the 803 keV γ ray and simultaneously uses the α measurement for normalization of the result and cancelation of the systematic errors. As it is seen in Table II and Fig. 5 the result of our measurement within its experimental uncertainty is in good agreement with the recommended nuclear data evaluations [16,25] and the experimental results obtained six decades ago.

In summary, the branching ratio for $^{210}\mathrm{Po}\rightarrow{}^{206}\mathrm{Pb}^{*}+\alpha\rightarrow{}^{206}\mathrm{Pb}+\gamma$, as compared to $^{210}\mathrm{Po}\rightarrow{}^{206}\mathrm{Pb}+\alpha$, was determined in this work by independent measurements of α and γ spectra of thin and thick bismuth samples simultaneously irradiated in a reactor. The branching ratio was found to be $(1.15\pm0.09)\times10^{-5}$, consistent with the results of the literature. As a by-product, a value of $\sigma=21.6\pm1.1$ mb was deduced for the $^{209}\mathrm{Bi}(n,\gamma)^{210g}\mathrm{Bi}$ thermal cross section by a measurement of the α-particle activity of ^{210}Po using the $^{197}\mathrm{Au}(n,\gamma)^{198}\mathrm{Au}$ cross section as a reference.

ACKNOWLEDGMENT

We would like to acknowledge the help of Dr. O. Girshevitz from Bar-Ilan University in measurements of the thickness of the bismuth foil sample with the RBS technique. We would like to thank Yaniv Tsarfati from Soreq NRC for his dedicated help in irradiating the bismuth samples.

[1] D. D. Clayton and M. E. Rassbach, Astrophys. J. **148**, 69 (1967).
[2] S. Halfon *et al.*, Rev. Sci. Instr. **85**, 056105 (2015).
[3] M. Tessler *et al.*, Phys. Lett. B **751**, 418 (2015).
[4] L. Weissman, M. Tessler, A. Arenshtam, I. Eliyahu, S. Halfon, C. Guerrero, B. Kaizer, D. Kijel, A. Kreisel, T. Palchan, M. Paul, A. Perry, G. Schimel, I. Silverman, A. Shor, N. Tamim, and S. Vaintraub, Phys. Rev. C **96**, 015802 (2017).
[5] A. Shor *et al.*, Phys. Rev. C **96**, 055805 (2017).
[6] M. A. Grace. R. A. Allen, D. West, and H. Halban, Proc. Phys. Soc. (London) **A64**, 493 (1951).
[7] M. Riou, J. Phys. Radium **13**, 244 (1952).
[8] R. W. Hayward, D. D. Hoppes, and W. B. Mann, J. Res. Natl. Bur. Standards **54**, 47 (1955).
[9] O. Rojo, M. A. Hakeem, and M. Goodrich, Phys. Rev. **99**, 112 (1955).
[10] A. Ascoli, M. Asdente, and E. Germanogli, Nuovo Cimento **4**, 946 (1956).
[11] N. S. Shmanskain, Sov. Phys. JETP **4**, 165 (1957).
[12] V. V. Ovechkin, Izvest. Akad. Nauk. SSSR Ser. Fiz. **21**, 1641 (1957).
[13] V. V. Ovechkin and E. M. Tsenter, Sov. J. At. Energ. **2**, 282 (1957).

[14] G. Bastin-Scoffier and R. J. Walen, C. R. Acad. Sci. **247**, 2333 (1958).
[15] T. Ohtsuki, J. Kasagi, N. Kasajima, H. Yamazaki, H. Yuki, M. Yukishima, and J. Radioanal, Nucl. Chem. **239**, 123 (1999).
[16] LNHB/CEA Table de Radionucleides, 2014, http://www.nucleide.org/DDEP.htm, http://www.nucleide.org/Laraweb/.
[17] Evochem GmbH, http://www.evo-chem.de.
[18] http://nano.biu.ac.il/.
[19] https://www.princetonscientific.com/high_purity_materials.php.
[20] A. Borella *et al.*, Nucl. Phys. A **850**, 1 (2011).
[21] http://www.ortec-online.com/products/radiation-detectors/germanium-hpge-radiation-detectors.
[22] http://www.geant.org/Projects/GEANT_Project_GN4.
[23] http://www.canberra.com/products/radiochemistry_lab/pdf/iSolo-SS-C39505.pdf.
[24] http://www.ezag.com/home/products/isotope_products/isotrak_calibration_sources/.
[25] E. Browne, Nucl. Data Sheets **88**, 3 (1999).
[26] F. G. Kondev, Nucl. Data Sheets **109**, 1527 (2008).